

## Research Article

# Theoretical Analysis and Experimental Study of Subgrade Moisture Variation and Underground Antidrainage Technique under Groundwater Fluctuations

Liu Jie, Hailin Yao, Pan Chen, Zheng Lu, and Xingwen Luo

State key Laboratory of Geomechanics and Geotechnical Engineering, Institute of Rock and Soil Mechanics, Chinese Academy of Science, Wuhan 430071, China

Correspondence should be addressed to Liu Jie; [liujie\\_whrsm@163.com](mailto:liujie_whrsm@163.com)

Received 22 May 2013; Revised 9 July 2013; Accepted 30 July 2013

Academic Editor: Ga Zhang

Copyright © 2013 Liu Jie et al. This is an open access article distributed under the Creative Commons Attribution License, which permits unrestricted use, distribution, and reproduction in any medium, provided the original work is properly cited.

Groundwater is a main natural factor impacting the subgrade structure, and it plays a significant role in the stability of the subgrade. In this paper, the analytical solution of the subgrade moisture variations considering groundwater fluctuations is derived based on Richards' equation. Laboratory subgrade model is built, and three working cases are performed in the model to study the capillary action of groundwater at different water tables. Two types of antidrainage materials are employed in the subgrade model, and their anti-drainage effects are discussed. Moreover, numerical calculation is conducted on the basis of subgrade model, and the calculate results are compared with the experimental measurements. The study results are shown. The agreement between the numerical and the experimental results is good. Capillary action is obvious when the groundwater table is rising. As the groundwater table is falling, the moisture decreases in the position of the subgrade near the water table and has no variations in the subgrade where far above the table. The anti-drainage effect of the sand cushion is associated with its thickness and material properties. New waterproofing and drainage material can prevent groundwater entering the subgrade effectively, and its anti-drainage effect is good.

## 1. Introduction

It is widely accepted that groundwater is an important factor impacting the highway structure in plateau area [1–3]. Climate environment and groundwater significantly impact the engineering properties of subgrade soil, as a result of repeated fluctuations of groundwater with the variation of atmospheric environment. In that situation, groundwater that migrates into the subgrade under capillary action not only causes long-term strength attenuation of subgrade soil but also produces large plastic deformation in early stage of subgrade. Capillary action, as a main external environmental factor, can influence the subgrade stability. Ground waterproof and drainage technology can reduce and control the capillary water effectively, and it becomes the key to design highway subgrade structure.

Recently, considerable studies have been conducted to investigate the groundwater fluctuations [4–10]. Great results have been achieved based on the numerical analysis. In

this paper, dynamic analysis on the law of subgrade moisture varying with groundwater fluctuations is conducted by numerical calculation, simplified analytical method, and laboratory model experiment. Two types of underground waterproofing and drainage materials are employed in the subgrade model, and their drainage effect are analyzed. Finally, the calculation and experiment results are contrasted.

## 2. Analysis of Subgrade Moisture Variation under Groundwater Fluctuations

Many studies [11–13] of groundwater fluctuations in the subgrade are based on numerical method; in this paper, the analytical method is introduced.

### 2.1. Basic Assumptions

- (1) The initial moisture of the subgrade is stationary; the subgrade soil is homogeneous and isotropic.

(2) The rising and falling courses of the groundwater table are consistent, respectively.

2.2. *Continuous Rising of Groundwater Table.* The rising and falling of groundwater in the subgrade are simplified to be a course of one-dimensional vertical seepage, and the water movement equation can be performed:

$$\frac{\partial \theta}{\partial t} = \frac{\partial}{\partial z} \left[ D(\theta) \frac{\partial \theta}{\partial z} \right] - \frac{\partial k(\theta)}{\partial z}, \quad (1)$$

where  $D(\theta)$  is diffusion coefficient,  $k(\theta)$  is permeability coefficient,  $t$  is time, and  $z$  is the height of the soil.

Boundary and initial conditions are as follows:

$$\begin{aligned} \theta &= \theta_0 & t = 0, & 0 \leq z \leq \infty, \\ \theta &= \theta_s & t > 0, & z = h = vt, \\ \theta &= \theta_0 & t > 0, & z = \infty, \end{aligned} \quad (2)$$

where  $v$  is rising speed of the groundwater,  $h$  is rising height of groundwater in time  $t$ .  $\theta_s$  is saturated water content,  $\theta_0$  is initial water content. Applying the Laplace transformation, (1) is solved;  $\theta(z, t)$  can be transformed:

$$\tilde{\theta}(z, p) = L(\theta(z, t)) = \int_0^{\infty} e^{-pt} \theta(z, t) dt, \quad (3)$$

and  $\partial \theta(z, t) / \partial t$  and  $\partial^2 \theta(z, t) / \partial z^2$  can be transformed:

$$\begin{aligned} L\left(\frac{\partial \theta(z, t)}{\partial t}\right) &= p\tilde{\theta}(z, p) - \theta(z, 0), \\ L\left(\frac{\partial^2 \theta(z, t)}{\partial z^2}\right) &= \frac{d^2 \tilde{\theta}(z, p)}{dz^2}. \end{aligned} \quad (4)$$

Equation (1) is converted to be image function ordinary differential equation:

$$D \frac{d^2 \tilde{\theta}(h, p)}{dh^2} - p\tilde{\theta}(h, p) + \theta_0 = 0. \quad (5)$$

By solving (5),  $\tilde{\theta}(z, p)$  is obtained:

$$\tilde{\theta}(z, p) = ae^{z\sqrt{p/D}} + be^{-z\sqrt{p/D}} + \frac{\theta_0}{p}, \quad (6)$$

where  $a, b$  is undetermined coefficient and  $p$  is Laplace transformation parameters.

Substituting (2) into (6),

$$\begin{aligned} a &= 0, & b &= \frac{\theta_s - \theta_0}{p} e^{h\sqrt{p/D}}, \\ \tilde{\theta}(z, p) &= \frac{\theta_s - \theta_0}{p} e^{(h-z)\sqrt{p/D}} + \frac{\theta_0}{p}. \end{aligned} \quad (7)$$

By checking the inverse Laplace transform table, the general expressions of subgrade moisture in arbitrary time and height under the condition of groundwater continuous rising are obtained:

$$\begin{aligned} \theta(z, t) &= (\theta_s - \theta_0) \operatorname{erfc} \frac{z - vt}{2\sqrt{Dt}} + \theta_0, & vt \leq z, \\ \theta(z, t) &= \theta_s, & vt > z. \end{aligned} \quad (8)$$

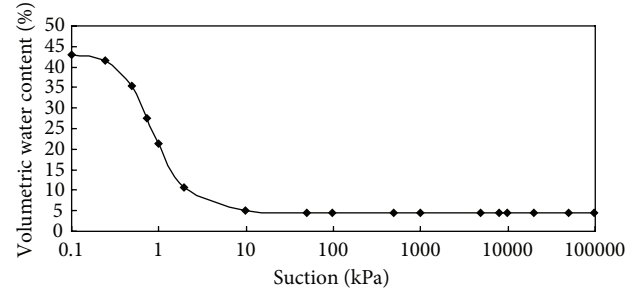


FIGURE 1: SWCC of sand subgrade.

2.3. *Continuous Falling of Groundwater Table.* The falling of groundwater meets the water movement equation (1); the boundary and initial conditions (2) are varied:

$$\begin{aligned} \theta &= \theta_0 & t = 0, & 0 \leq z \leq \infty, \\ \theta &= \theta_s & t > 0, & z = h_0 - vt, \\ \theta &= \theta_0 & t > 0, & z = \infty. \end{aligned} \quad (9)$$

The height of the initial groundwater table is  $h_0$ ; the other symbols are the same to (2). Substituting (9) into (6), the general expression of subgrade moisture in arbitrary time and height under the condition of groundwater continuous falling is obtained:

$$\theta(z, t) = (\theta_s - \theta_0) \operatorname{erfc} \left( \frac{vt + z - h_0}{2\sqrt{Dt}} \right) + \theta_0. \quad (10)$$

2.4. *Numerical Example.* There is a sand subgrade; the height of the subgrade is 2 m, and the depth of the groundwater table is 1 m. The rising and falling speed of groundwater table is 0.0002 m/s, and its duration is 60 min. Soil and water parameters are shown in Figure 1.

Design and monitor programs of the experiment are shown in Figure 9. There are three working cases in three model boxes.

Variation of subgrade moisture in the rising and falling course of groundwater table can be seen in Figures 2 and 3. The numerical and analytical calculation results of subgrade moisture variations under groundwater fluctuations are compared in Figure 4. As the groundwater is rising, the capillary action of groundwater is obvious. In the tenth minutes, capillary water rises to 0.45 m, and in the sixth ten minutes, the capillary water rises to 1.7 m. As the groundwater is falling, subgrade moisture in the position near the groundwater table decreases rapidly, but it has no variations in the position far above the groundwater table; that is, because part of the capillary water cannot be discharged timely in a short time and still strands in the pores. The agreement between numerical and analytical methods solving subgrade moisture variations under groundwater fluctuations is good. It is reasonable and practicable using analytical method to obtain the subgrade moisture considering groundwater fluctuations.

TABLE 1: Basic soil properties of Hongshan clay.

| Natural density/(g/cm <sup>3</sup> ) | Nature water content/% | Specific gravity/(g/cm <sup>3</sup> ) | Plastic limit/% | Liquid limit/% | Maximum dry density/(g/cm <sup>3</sup> ) | Optimum water content/% |
|--------------------------------------|------------------------|---------------------------------------|-----------------|----------------|--|-------------------------|
| 1.386                                | 21.8                   | 2.76                                  | 21.11           | 43.42          | 1.88                                     | 15.7                    |

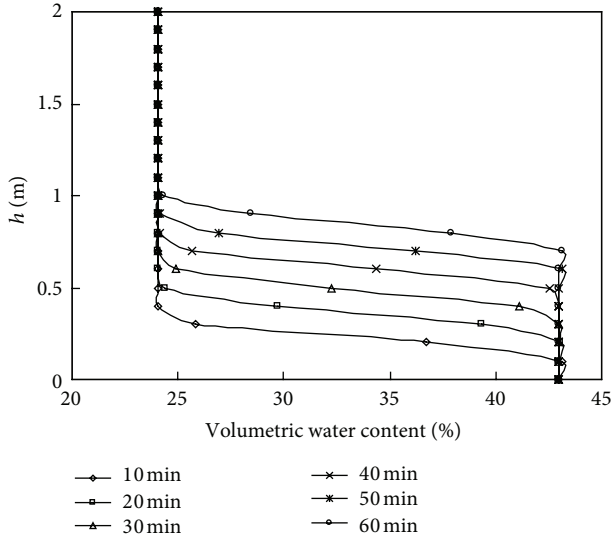


FIGURE 2: Variation of subgrade moisture in the rising course of groundwater table.

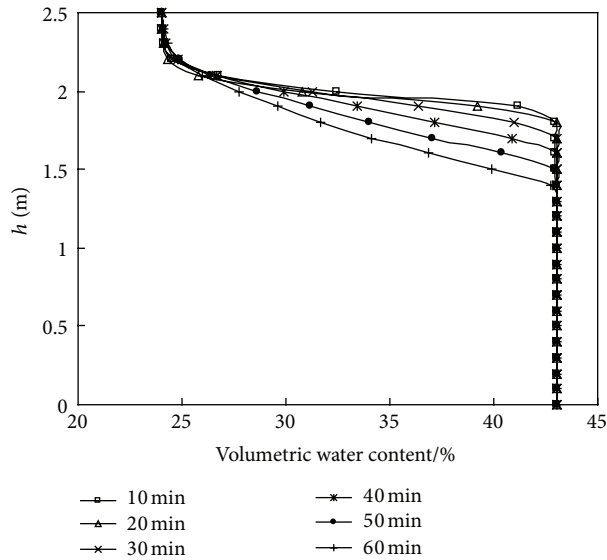


FIGURE 3: Variation of subgrade moisture in the falling course of groundwater table.

### 3. Laboratory Model Experiment

3.1. *Laboratory Experimental Analysis for Basis Properties and Soil-Water Features of Hongshan Clay.* The experimental soil is Hongshan clay; it is typical viscous soil. Table 1 lists its basis physic properties. The natural water content of Hongshan clay

is close to its plastic limit and larger than its optimum water content.

3.2. *Introduction of SWCC Experiment.* The SWCC experiment of Hongshan clay is preparing for the laboratory subgrade model experiment; the experimental instruments are composed of air supply system, penetration instrument, control panel, a constant flow rate maintain system, weighing system, and data acquisition system. The main instruments are shown in Figures 5 and 6.

The diameter of the sample is 5.12 cm; its height is 2.83 cm. The initial water content of the sample is 15.7%, the compactness of the sample is 85 percent of maximum dry density obtaining from Table 1, and the sample is saturated. Different values (5 kPa, 10 kPa, 25 kPa, 50 kPa, 75 kPa, 100 kPa, 150 kPa, 200 kPa, 300 kPa, and 400 kPa) of air pressure are applied progressively on the sample; the weight of discharged water is recorded every day. The water content of the sample is obtained by calculating the discharged water under different air pressures. The step of pressurization, drainage, and weighing is repeated in the process of the experiment, and the SWCC of Hongshan clay is obtained.

The water content obtained from the experiment is mass water content  $\theta_w$ , the conversion relation between volumetric water content  $\theta_v$  and mass water content  $\theta_w$  is  $\theta_v = \theta_w \cdot \rho$ , and the SWCC represented by volumetric moisture can be got.

Normally, SWCC meets an empirical formula like V-G model, Fredlund-Xing model, and so on. The V-G model is used in this paper, it is

$$\frac{\theta - \theta_r}{\theta_s - \theta_r} = \left( \frac{1}{1 + (\alpha h)^n} \right)^m, \tag{11}$$

$$\left( m = 1 - \frac{1}{n}, 0 < m < 1 \right),$$

$r, \theta, r$ : empirical coefficients,  $\theta_r$ : residual water content (cm<sup>3</sup>/cm<sup>3</sup>);  $\theta_s$ : saturated water content (cm<sup>3</sup>/cm<sup>3</sup>);  $\theta$ : soil water content (cm<sup>3</sup>/cm<sup>3</sup>).

The permeability function is also based on V-G model:

$$k_w = k_s \frac{\left[ 1 - (a\psi^{(n-1)}) (1 + (a\psi^n)^{-m}) \right]^2}{((1 + a\psi^n)^n)^{m/2}}. \tag{12}$$

The empirical coefficients in V-G model are got:  $a = 0.021 \text{ kPa}^{-1}$ ;  $n = 1.27$ ;  $m = 0.2126$ ; the saturated permeability coefficient is  $k_s = 4.74 \times 10^{-9} \text{ m/s}$ . The comparison of SWCC got by experiment and VG model is shown in Figure 7.

3.3. *Laboratory Subgrade Model Experiment.* The Laboratory subgrade model is built in a plexiglass box with a length of

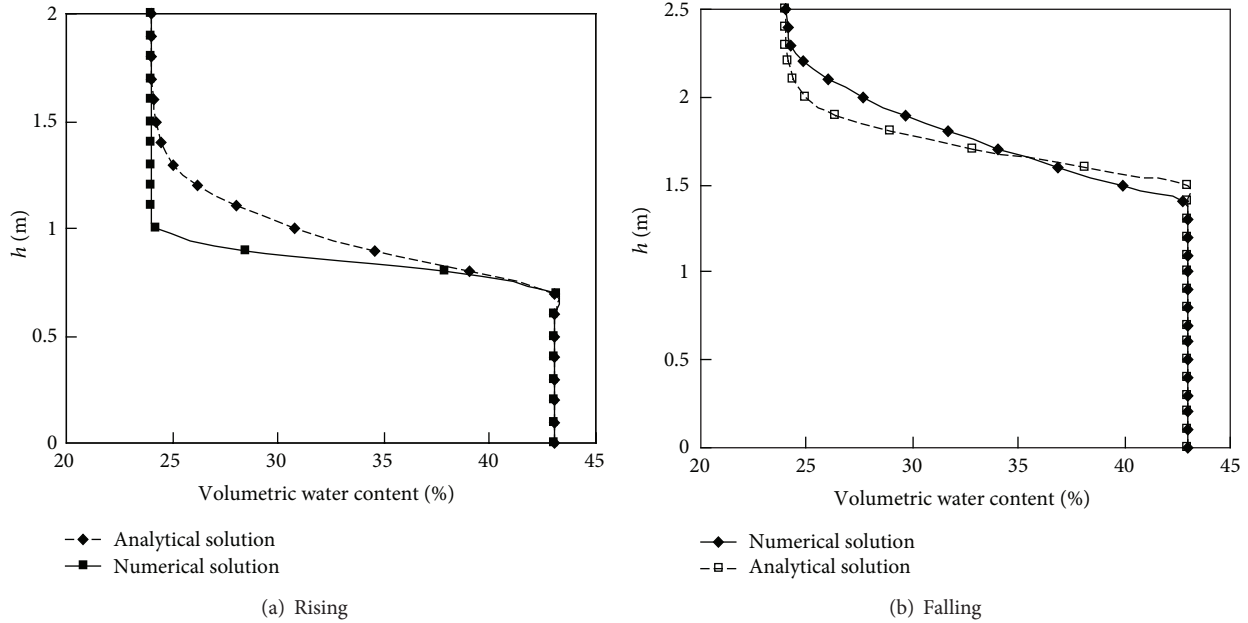


FIGURE 4: Comparison of numerical and analytical methods for solving subgrade moisture variations under groundwater fluctuations.



FIGURE 5: Outlet and evaporation correction bottle.



FIGURE 6: Servo flow permeameter.

2.4 m, a width of 0.8 m, and a height of 1.6 m. It is divided into 3 same boxes along the lengthwise direction, and the filling height of soil is 0.8 m in each box. A layer of gravel is laid at the bottom of the model to speed up the seepage of the groundwater, which thickness is about 10 cm; permeable geotextiles are laid at the top and bottom surface of the gravel, and they cannot only prevent the fine-grained soils falling into the gravel pores influencing the seepage of groundwater, but also prevent the gravel piercing the model box during soil compaction process.

The experiment device is composed of plexiglass box, water tank, and measurement acquisition apparatus. Hongshan clay is used as subgrade/foundation filling material, and groundwater table is controlled by adjusting the water level in the water tank. The design process of water fluctuations is set as 0.1 m  $\rightarrow$  0.3 m  $\rightarrow$  0.5 m. Experiment temperature is kept at  $(25 \pm 2^\circ\text{C})$ . The duration of groundwater table in each height

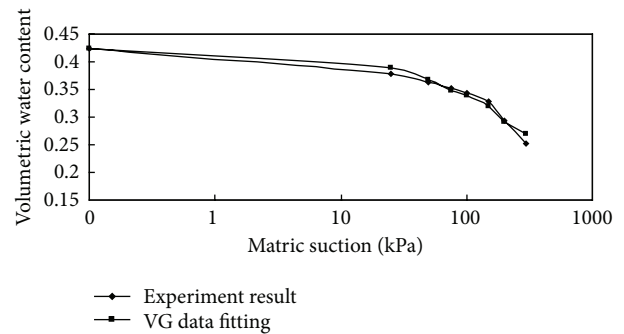


FIGURE 7: SWCC of Hongshan clay.

is 60 d, 100 d, and 100 d. The initial mass moisture content of subgrade model filling is 21.5%, and its compaction degree is 85%.

TABLE 2: Conversion relationship of mass and volumetric water content got from the moisture probes.

| Mass water content/% | Volumetric water content got from the moisture probes/% |       |       |       |       |       |      |      |      |
|----------------------|---|-------|-------|-------|-------|-------|------|------|------|
|                      | 1-1#  | 1-2#  | 1-3#  | 2-1#  | 2-2#  | 2-3#  | 3-1# | 3-2# | 3-3# |
| 18.4                 | 31.9  | 30    | 30    | 30.44 | 29.4  | 30.21 | 26.8 | 27.7 | 27.9 |
| 19.5                 | 33.5  | 33    | 33    | 30.35 | 29.83 | 31.89 | 33.2 | 29.3 | 29.8 |
| 21.6                 | 35  | 36    | 34.58 | 35.28 | 33.63 | 34.82 | 34.7 | 32.7 | 33.9 |
| 23.55                | 38.6  | 38.2  | 36.91 | 37.76 | 36.28 | 39.21 | 36.1 | 35.1 | 36.3 |
| 24.92                | 39.2  | 40.01 | 39.88 | 39.52 | 39.15 | 40.64 | 38.8 | 38.8 | 39.2 |

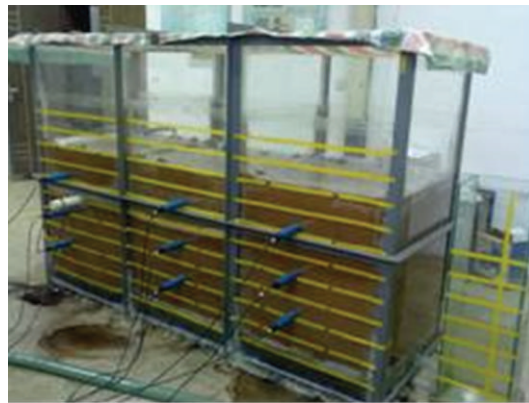


FIGURE 8: Subgrade model.

Water content is monitored once per hour in each model box using water content probes (accuracy =  $\pm 2\%$ , monitor range =  $0\sim 100\%$  ( $\text{m}^3/\text{m}^3$ )). The probes are set at 0.3 m, 0.5 m, and 0.7 m in height. Since the data got from the water content probes is mass water content, it is needed to be converted to volumetric water content. The conversion relationship is presented in Table 2.

Fitting formulas of mass and volumetric water content for each probe are

$$1-1\#:y = 1.155x + 0.1069, 1-2\#:y = 1.4618x + 0.0388, 1-3\#:y = 1.3612x + 0.054793,$$

$$2-1\#:y = 1.5178x + 0.018915, 2-2\#:y = 1.5271x + 0.006819, 2-3\#:y = 1.651x - 0.0031,$$

$$3-1\#:y = 1.5182x + 0.0114, 3-2\#:y = 1.631x + 0.024993, 3-3\#:y = 1.6998x - 0.032638,$$

where  $x$  is mass water content and  $y$  is volumetric water content.

The subgrade model is shown in Figure 8.

*Case 1* (box 1). The height of the foundation is 0.6 m; the height of the subgrade is 0.3 m, there has no drainage facilities.

*Case 2* (box 2). The height of the foundation is 0.6 m; the height of the subgrade is 0.3 m; and waterproof sand cushion (about 10 cm thick) is set between the foundation and subgrade.

*Case 3* (box 3). The height of the foundation is 0.6 m; the height of the subgrade is 0.3 m; a layer of new antidrainage

material, that is, plastic film and plastic drainage plate, is set between foundation and subgrade.

Plastic film is used to prevent the groundwater rising into the subgrade, and plastic drainage plate is employed as a drainage path of water in the subgrade. Plastic film is placed on the plastic drainage plate, which is laid on the foundation, and they are compacted. Some drain holes are drilled in the position of plastic drainage plate in the box, in order to promote the discharge of groundwater. Figure 10 shows the details of the new antidrainage material.

## 4. Analysis of Experiment Results

*4.1. The Tendency of Moisture Variations of Subgrade Model.* Variations of subgrade moisture in model boxes 1, 2, and 3 are shown in Figure 11. In Stage 1, the groundwater table is at the height of 0.1 m, and the variation tendency of subgrade moisture is consistent at the height of 0.3 m in three boxes; there are some increases in moisture at the beginning of the experiment, but the variation rate gradually slows as the experiment going on. At the height of 0.5 m, which is far above the groundwater table, the moisture in the subgrade has no variations. After a period of time, the capillary water rises and enters into the interior of subgrade. Subgrade moisture above the water table begins to increase continuously in three boxes. But at the height of 0.7 m, the subgrade moisture in boxes 2 and 3 has no variations. That is, because the thick waterproof sand cushion and antidrainage material are set respectively in boxes 2 and 3, capillary water is prevented from entering the subgrade. From

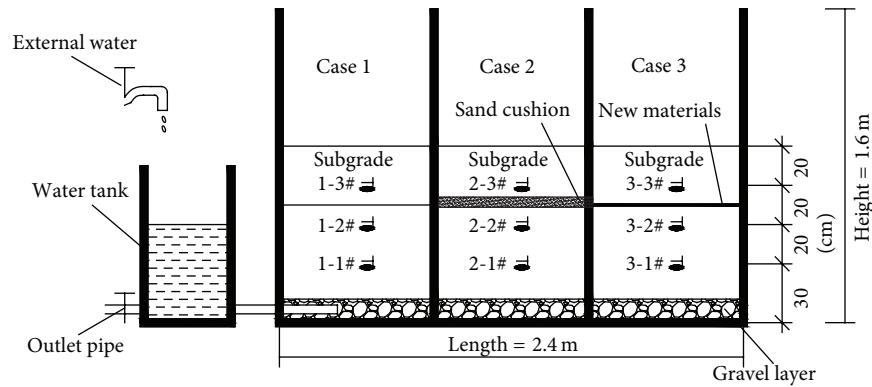


FIGURE 9: Schematic cross-section of subgrade model.

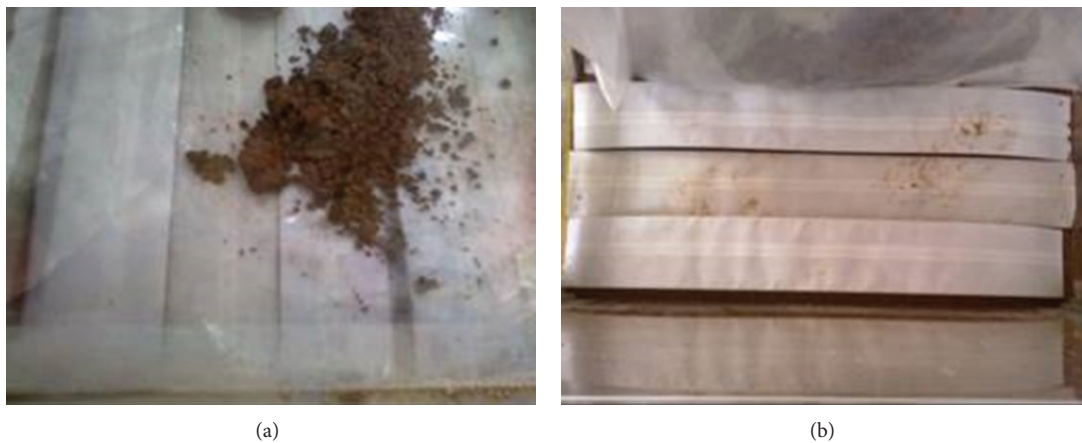


FIGURE 10: New antidrainage material.

the experiment result, it can be concluded that when the groundwater table is low, thick waterproof sand cushion and antidrainage material can play a good role in waterproof and drainage.

In Stage 2, the groundwater table rises to the height of 0.3 m. The moisture of the subgrade below the water table reaches saturated moisture in three model boxes. In 1# model box, the path of capillary water rising to the higher subgrade is shorter than that in Stage 1. Consequently, the subgrade moisture rises from 35.02% to 40.85% at the height of 0.7 m. In 2# model box, waterproof sand cushion inside the model keeps some water out of the upper subgrade. Due to the maximum rising height of the capillary water that is higher than the thickness of the sand cushion, the sand cushion cannot keep all of the capillary water out of the internal subgrade, and subgrade moisture varies from 32.85% to 34.72% at the height of 0.7 m. In 3# model box, antidrainage material unleashes a good antidrain effect; the subgrade moisture in the position above the material has no variations.

In Stage 3, the groundwater table rises to 0.5 m. In 1# model box, the subgrade moisture above the water table has no variations, since the subgrade moisture has varied completely in the prophase, and it would not vary at this

stage. In 2# model box, the sand cushion has no antidrainage effect completely in this stage. Subgrade moisture varies significantly at the height of 0.7 m. In 3# model box, the subgrade moisture in the position above the water table still has no variations, and it can be proved that the new antidrainage material has good antidrainage effect.

**4.2. Comparison of Numerical Calculated Subgrade Moisture with Experimental Results.** In this paper, we focus on the subgrade moisture variations under the capillary action of the groundwater, so we did not do any physical properties experiments for the waterproof sand cushion in Case 2. Meanwhile, it is difficult to obtain the properties and permeability of the plastic drainage plate by conventional laboratory experiment, so, the analysis is conducted only in Case 1.

*Stage 1.* Groundwater table stays at the height of 0.1 m, and its duration is 60 d.

*Stage 2.* Groundwater table rises from the height of 0.1 m to 0.3 m, and its duration is 100 d.

*Stage 3.* Groundwater rises from the height of 0.3 m to 0.5 m, and its duration is 100 d.

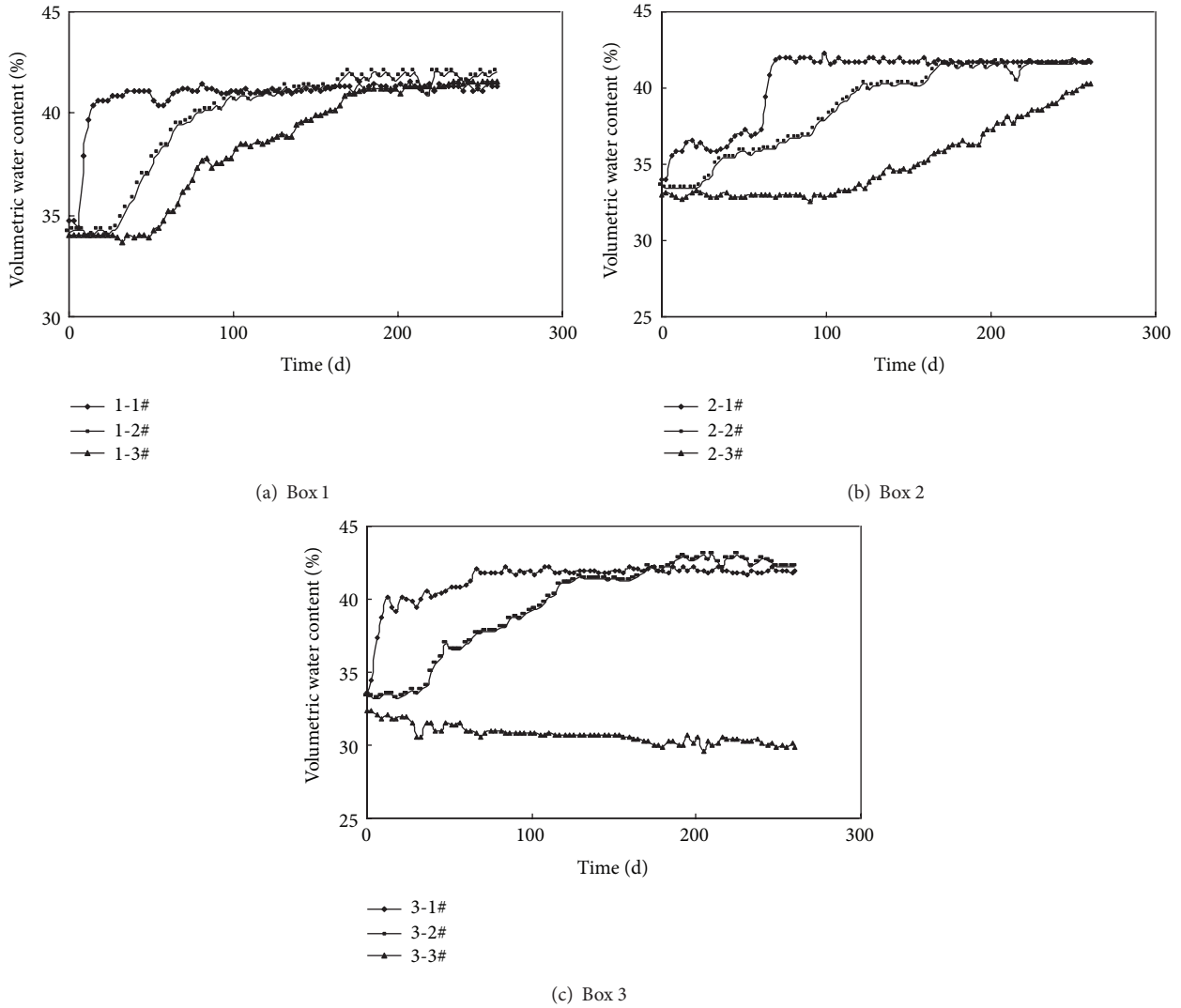


FIGURE 11: Variations of subgrade moisture in model boxes 1, 2, and 3.

Comparisons of calculated subgrade moisture with experimental results in different stages are shown in Figures 12, 13, and 14. During the process of numerical calculation analysis, the soil water parameters are obtained by SWCC experiment, and its results are precise and not affected by some factors like (environment, initial water content, compaction effects, etc.), the saturation level of the soil got from the model experiment is less than that got from SWCC experiment, but it does not affect the reliability to study the vary trends of the subgrade moisture using laboratory model experiment. The vary trends of subgrade moisture considering groundwater fluctuations which obtained by laboratory model experiment and numerical calculation are consistent.

**5. Conclusions**

Subgrade moisture increases constantly under the capillary action in the process of groundwater continuous rising, and

the variation of the subgrade moisture with the time is significant. In the process of the groundwater continuously falling, the subgrade moisture decreases near the groundwater table and has no variations far above the groundwater table.

The results obtained from the laboratory subgrade model experiment show that sand waterproof cushion can prevent water from entering the upper subgrade when the groundwater is low, but its blocking effect is associated with its material properties, thickness, and the height of the groundwater table. New antidrainage material can completely prevent capillary water from entering the entire range of subgrade, and it has effective antidrainage function.

Although there are many factors affecting the results in the experimental process, a good consistence is obtained between laboratory model experiment and numerical calculation of the moisture variations in subgrade considering groundwater fluctuations. It can be concluded that the subgrade moisture migration law can be well reflected by laboratory subgrade model experiment.

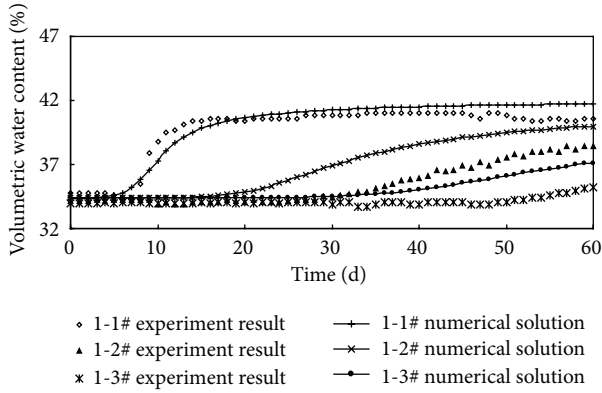


FIGURE 12: Comparison of calculated subgrade moisture with experimental results in Stage 1.

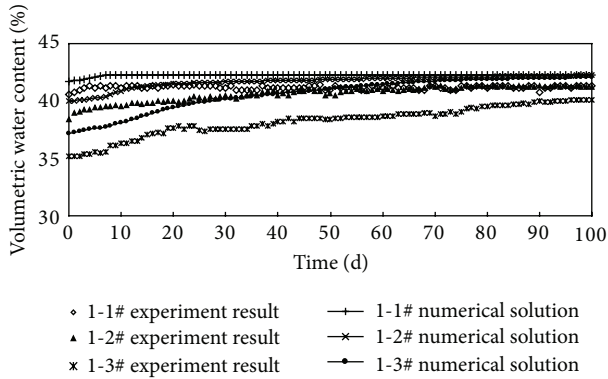


FIGURE 13: Comparison of calculated subgrade moisture with experimental results in Stage 2.

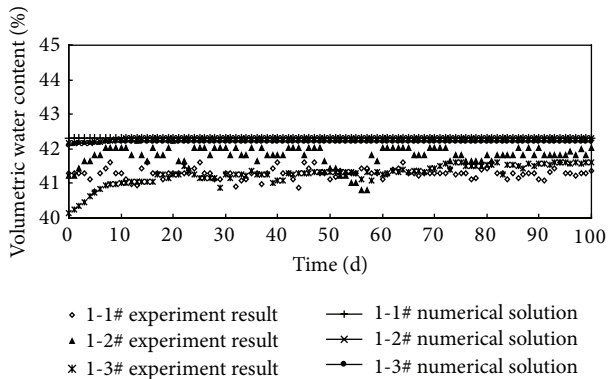


FIGURE 14: Comparison of calculated subgrade moisture with experimental results in Stage 3.

## Acknowledgments

The authors gratefully acknowledge the financial support of the National 973 Project of China (no. 2013CB036405) and the Natural Science Foundation of China (nos. 51209201 and 51279198).

## References

- [1] A. R. Kacimov, Y. V. Obnosov, and J. Perret, "Phreatic surface flow from a near-reservoir saturated tongue," *Journal of Hydrology*, vol. 296, no. 1-4, pp. 271-281, 2004.
- [2] A. W. Warrick, P. J. Wierenga, and L. Pan, "Downward water flow through sloping layers in the vadose zone: analytical solutions for diversions," *Journal of Hydrology*, vol. 192, no. 1-4, pp. 321-337, 1997.
- [3] G.-C. Zhang, H.-M. Tang, and B. Hu, "Study of influence of unsaturated seepage on stability of landslide," *Rock and Soil Mechanics*, vol. 28, no. 5, pp. 965-970, 2007.
- [4] D.-M. Sun, Y.-M. Zhu, and M.-J. Zhang, "Research on unsteady seepage problem of bank slope due to drawdown of reservoir water level," *Rock and Soil Mechanics*, vol. 29, no. 7, pp. 1807-1812, 2008.
- [5] W.-K. Feng, Y.-C. Shi, H.-J. Chai, H.-C. Liu, and F. Ji, "The simplified solution of phreatic saturation line under the actions of rainfall and reservoir water level fluctuation," *Journal of Chengdu University of Technology*, vol. 33, no. 1, pp. 90-94, 2006.
- [6] Q. Liu, Z. Zhu, X. He, G. Lu et al., "Unsaturated seepage analysis of the influence of water level fluctuation on pore water pressure of landslide in reservoir area," *Rock and Soil Mechanics*, vol. 29, pp. 85-89, 2008.
- [7] J. M. Gasmo, H. Rahardjo, and E. C. Leong, "Infiltration effects on stability of a residual soil slope," *Computers and Geotechnics*, vol. 26, no. 2, pp. 145-165, 2000.
- [8] D. G. Fredlund and A. Xing, "Equations for the soil-water characteristic curve," *Canadian Geotechnical Journal*, vol. 31, no. 4, pp. 521-532, 1994.
- [9] D. G. Fredlund, A. Xing, M. D. Fredlund, and S. L. Barbour, "The relationship of the unsaturated soil shear strength to the soil-water characteristic curve," *Canadian Geotechnical Journal*, vol. 32, pp. 521-532, 1995.
- [10] T. L. Zhan and N. W. Charles, "Analytical analysis of rainfall infiltration mechanism in unsaturated soils," *International Journal of Geomechanics*, vol. 4, no. 4, pp. 273-284, 2004.
- [11] Y. Zhang and X. Hu, "Calculation of saturation line of groundwater under reservoir water table uniform rising," *Hydrogeology and Engineering Geology*, no. 5, pp. 46-49, 2007.
- [12] Q. Wu and Z. Lin, "Analytic solutions for shallow water table in inclined and layered slope under drawdown condition," *Geological Science and Technology Information*, vol. 26, no. 2, pp. 91-92, 2007.
- [13] Q. Wu, H.-M. Tang, L.-Q. Wang, and Z.-H. Lin, "Analytic solutions for phreatic line in reservoir slope with inclined impervious bed under rainfall and reservoir water level fluctuation," *Rock and Soil Mechanics*, vol. 30, no. 10, pp. 3025-3031, 2009.